Finite Element Analysis of PCCP Curling and Roughness

Zahidul Siddique[1], Ph.D. and Mustaque Hossain[2], Ph.D., P.E.

Abstract

Smoothness specifications for newly built Portland Cement Concrete Pavements (PCCP) in Kansas have evolved over the last two decades through applications and a number of revisions. However, some PCCP sections built under current specifications in the smoothness bonus range experience rapid loss of smoothness with time. Sometimes this happens even before the sections are opened to traffic. It is believed that this loss results from curling due to the temperature differential between the pavement top and bottom surfaces. In this study, three-dimensional simulation of curling of PCCP has been presented using a finite element (FE) software, ANSYS. A number of FE models were built to simulate several newly built PCCP sections in Kansas. The sections were modeled as three-layer systems with cement-treated base and lime-treated subgrade. Layer materials were modeled as linear elastic and the properties were obtained from the tests conducted during construction. Pavement layers and steel dowel bars were modeled using 3-dimensional solid (brick) elements. The complex interaction of the slab with the dowel bars was modeled as a contact problem. Regression models were developed for the curling deflection and International Roughness Index (IRI), a roughness statistics resulting from the curled profiles, based on different simulation parameters. The results obtained from the simulations show that the curling deflection and IRI calculated from the deflected slab profiles are affected by the slab thickness, compressive strengths of the concrete slab and base layers, and the temperature differential between the pavement top and bottom surfaces. Both curling deflection and IRI increase with an increase in temperature differential and compressive strength of the stabilized base layer. Higher slab thickness and concrete compressive strength would result in lower curling deflection and IRI values.

Introduction

Smoothness specifications for newly built Portland Cement Concrete Pavement's (PCCP) in Kansas have evolved over the last 20 years through applications and a number of revisions. The first PCCP with smoothness specification was built by the Kansas Department of Transportation (KDOT) in 1985, and the first specifications for as-constructed smoothness were adopted in 1990 (Parcells and Hossain, 1994). Changes to the original specifications of 1990 are considered to have enhanced the quality of new pavement construction in Kansas. However, early life (one to two years after construction) roughness increase on some newly built concrete

[1] McMahon Associates, Inc., 7741 N Military Trail, Palm Beach Gardens, FL 33410, Zahidul.Siddique@mcmtrans.com
[2] Dept. of CE, 2118 Fiedler Hall, Kansas State University, Manhattan, KS 66506, mustak@ksu.edu

pavements was quite noticeable. Every year approximately $1.5 million is paid as potential smoothness bonus in Kansas. Some of these sections experience rapid loss of smoothness with time. Sometimes this happens even before the sections are opened to traffic. Similar trends were also observed in Arizona and South Dakota. It is believed that this significant smoothness loss results from curling. In addition to smoothness loss due to physical deformation of slab, curling induces stress in the pavement slab. This stress can be a significant factor in contributing to early pavement cracking (Tang et al., 1993). Recently it has been reported that some concrete pavement slabs are built with "locked in" curvature, a physical phenomenon due to uneven shrinkage caused by nonuniform temperature rise and non-uniform curing (Byrum, 2000). Thick slabs, with top faces exposed during curing, will generally curl up on the ends because of drying shrinkage. This curling could affect future strength development and performance of concrete pavements. Because pavements are typically constructed during daytime, the temperature gradients during construction also tend to cause upward curling. Yu et al. (1998) showed that the average magnitude of built-in curling is about 1^0F/in. for pavements in wet-freeze climate. The combination of built-in curling and actual temperature gradients can cause significant upward curling of the slabs during nighttime.

Finite Element Analysis of PCCP

Finite element method (FEM) has been used in pavement engineering for decades. Many researchers have modeled the response of rigid pavement systems to applied static, dynamic and thermal loadings. This section describes some of the past PCCP studies using FEM. Initially, two-dimensional finite element programs that rely on plate elements to discretize the pavement slabs and base layers were developed. These programs attempted to capture some of the more complex aspects of the behavior of rigid pavement slabs, such as, dowel-concrete interaction, aggregate interlock, and loss of subgrade support. Tabatabaie and Barenberg (1978) developed the program ILLI-SLAB, which incorporates all of these behaviors. The program JSLAB (Tayabji and Colley, 1986) allows dowel-slab interaction to be modeled by treating the dowel as a beam on elastic foundation. Both WESLIQID (Chou, 1981) and KENSLABS (Huang, 1993) use two-dimensional (2D) thin plate elements to model the concrete slab on a dense liquid foundation. Recently several other FE-based computer programs have been developed. Chatti et al. (1994) developed a dynamic FE computer program, DYNA-SLAB, for the analysis of jointed concrete pavements subjected to moving transient loads. EverFE developed by Davis et el. (1998) is a three-dimensional (3D) FE rigid pavement analysis tool, which considers aggregate interlock, dowel-aggregate interlock, and loss of subgrade support. Temperature effect is also considered. 3DPAVE (Kuo, 1994) explores many complicated effects and interactions in concrete pavements, including foundation support, base thickness, stiffness, and interface bond/friction; slab curling and warping due to temperature and moisture gradients, dowel and aggregate interlock load transfer action at joints; and improved support with a widened lane, widened base, or tied concrete shoulder. Some of these programs are based on the idealization of the pavement as a slab on either Winkler or elastic foundation.

Rather than developing custom-mode FE programs, many researchers have also used commercially available FE software to build concrete pavement models (Saxena and Dounias, 1986). Since the computer capacity and speed have improved significantly, use of commercially available software seems more realistic and economic. These programs include ABAQUS and ANSYS. The former one has been widely used by the researchers in the area of pavement engineering (Kuo, 1994; Uddin et al., 1995; Vepa and George, 1997). One of the disadvantages of this type of analysis is that the large aspect ratio (ratio of the largest dimension to the least dimension of a finite element, which ideally should be unity) problems. Also, a proper representation of the stress gradient across the depth can only be achieved with three to four layers of elements throughout the depth (Channakeshava et al., 1993). For these reasons, a large number of finite elements are needed, and that makes the problem computationally expensive.

Objective

The objective of this study is to present finite element simulation of curling of Portland cement concrete pavements. The study also investigates the effect of curling on the roughness/smoothness of PCCP.

Test Section and Data Collection

Twelve newly built PCCP sections located on Interstate routes 70 and 135 in Kansas were selected for the study. The sections were constructed in the summer of 2000 and 2001. Concrete pavements in Kansas are three-layer systems. All test sections are jointed plain concrete pavements (JPCP) with 5 m (16.4 ft) joint spacing and steel dowel bars. The thickness of the concrete slab varies between 250 mm (10 in.) and 315 mm (12.5 in.). All sections were built over 100 mm (4 in.) cement-treated drainable base (known as bound drainable base or BDB in Kansas) and 150 mm (6 in.) lime-treated subgrade. The 28-day compressive strengths of BDB ranged from 860 kPa to 4,480 kPa (125 to 650 psi). The concrete mixtures consisted of either 40% coarse and 60% fine aggregates or 45% coarse and 55% fine aggregates. Average 28-day core compressive strength was in between 27 and 44.5 MPa (3,950 to 6,450 psi) and the 3-day modulus of rupture varied from 3.3 to 4.4 MPa (480 to 630 psi). Table 1 presents the slab thicknesses and material properties for the test sections. As the study deals with curling, temperature was used as loading. Temperature of the bottom of the concrete slab was collected with thermocouples, whereas that of the slab top was collected with a hand-held infrared thermometer. All temperature data were collected hourly during the day of construction. Figure 1 presents the temperature variation between the pavement top and bottom surfaces throughout the day of construction for Sections 11 and 12. The figure shows that a high temperature differential exists between the pavement top and bottom throughout the day. For most hours of the day, temperature at the top of the slab is higher than that of the bottom, but at around 7:00 P.M., temperature at the bottom exceeded that at the top.

Table 1. Slab Thickness and Material Properties of Test Sections

Section	Slab Thickness (mm)	% Aggregate in Mix		% Air	Water-Cement Ratio	BDB Compressive Strength (MPa)	Concrete Compressive Strength (MPa)
		Coarse	Fine				
1	315	40	60	6.50	0.49	0.90	31.7
2	315	40	60	6.50	0.49	0.90	31.7
3	280	45	55	7.00	0.45	1.93	44.5
4	280	45	55	7.00	0.45	2.24	44.5
5	290	45	55	7.50	0.47	4.44	41.4
6	290	45	55	7.50	0.47	4.10	41.4
7	315	40	60	6.50	0.42	N/A*	28.2
8	315	40	60	6.50	0.42	N/A*	27.2
9	250	40	60	6.75	0.41	1.56	32.5
10	250	40	60	6.75	0.41	2.17	32.5
11	300	40	60	5.25	0.41	1.08	35.9
12	300	40	60	5.25	0.41	1.49	35.9

* samples crumbled before testing

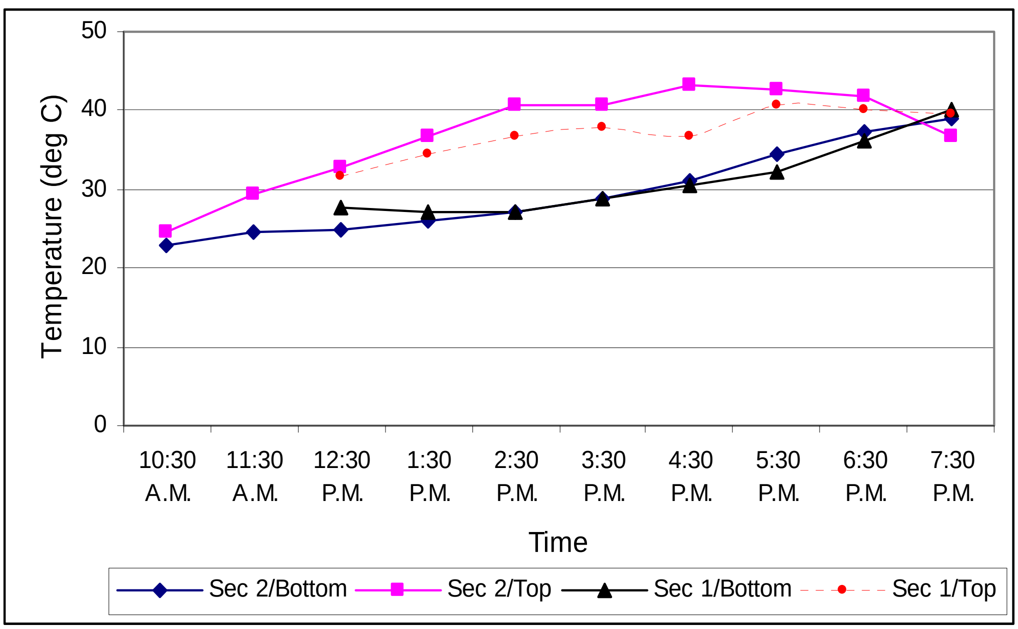

Figure 1. Typical Temperature Variation of a Freshly Poured Concrete Pavement Slab

Finite Element (FE) Modeling

Twelve (12) three-dimensional FE models were built using a commercially available FE software program ANSYS (2003) to simulate the test sections in this study. Each model was built with the actual geometric proportions and material properties from the study sections.

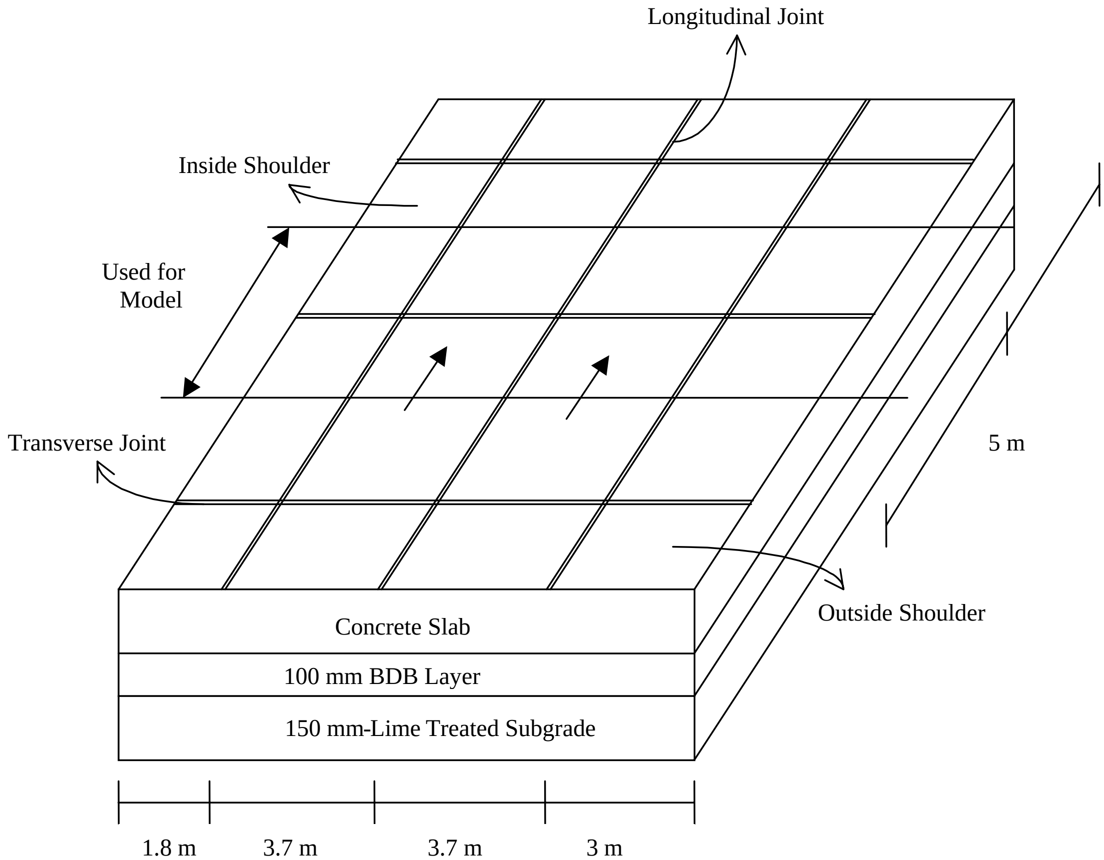

Figure 2. Model Geometry Used in the Study

Geometry

As shown in Figure 2, the concrete pavement was modeled as a three-layer system: concrete slab with varying thickness, 100 mm (4 in.) BDB layer, and 300 mm (6 in.) treated subgrade layer. Each model consists of both driving and passing lanes as well as two shoulders (inside and outside). Each lane is 3.7 m (12 ft) wide, whereas the widths of the inside and outside shoulders are 1.8 m (6 ft) and 3 m (10 ft), respectively. All lanes and shoulders are separated by longitudinal joints with width of 9.5 mm (3/8 inch) and a depth equal to the quarter of the slab thickness. Transverse joints in the model are located at 5 m (approximately 16.4 ft) intervals and the dimensions are the same as those of the longitudinal joints. Cracks developing along the slab edge under the transverse joints were also modeled. Dowel bars (not shown in the figure), located at the mid-depth of the slab with a bar diameter of 37.5

mm (1.5 inch) and length of 450 mm (18 in.), were placed at 300 mm (12 in.) intervals. Dimensions and spacing of the dowel bars were the same for all test sections. Because of the symmetry in the longitudinal (driving) direction, one half of the slabs on both sides of a transverse joint were used as the model geometry.

Element

Element selection is vital in obtaining reasonable results in the FE analysis. Based on the experiences of previous researchers (Channakeshava, 1993; Kuo, 1994; Davis et al., 1998), a 3-D 20-node brick element was selected as the candidate element for this study. In the ANSYS library, this element is known as SOLID186 (ANSYS, 2003). Figure 3 shows a SOLID186 element. The element is defined by 20 nodes, each with three degrees of freedom: translations in the nodal x, y, and z directions. It supports plasticity, hyperelasticity, creep, stress stiffening, large deflection, and large strain capabilities. The interaction between concrete and the dowel bars is a complex one. This interaction was modeled as a contact problem. Rigid-to-flexible type of contact, available in the ANSYS library, was used in "surface-to-surface" contact mode. Target element TARGE170 and contact element CONTA174 were selected to model the target and contact surfaces, respectively. Figure 4 shows the geometry and node locations of the CONTA174 element. It is defined by eight nodes (the underlying solid or shell element has midside nodes).

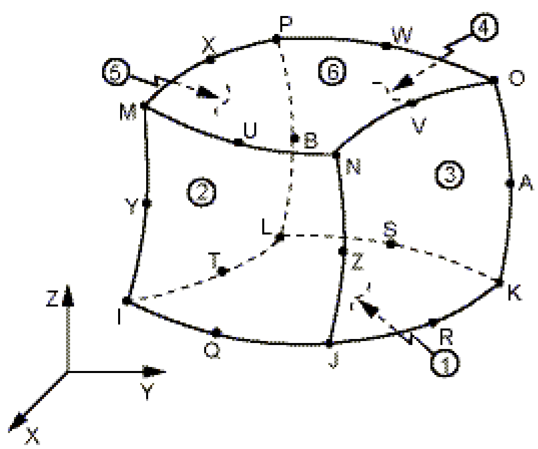

Figure 3. SOLID186 Element

Material Properties

Concrete layer material was modeled as linear elastic. The effect of concrete slab on curling is overwhelming compared to the effects due to the base and subgrade layers. Hence, base and lime-treated subgrade layers were also modeled as linear elastic. Material properties needed for the FE model include the elastic properties, such as, Modulus of Elasticity and Poisson's ratio of different layers. Since this study deals with curling, which is caused by temperature, another important material property that was needed is the coefficient of thermal expansion. Modulus of elasticity values for the concrete and BDB layers were obtained from the empirical relationship between the modulus of elasticity and the compressive strength of concrete. The relationship used in this study is given by the American Concrete Institute (ACI) Building Code (ACI, 1986) as

$$E_c = 57000\sqrt{f_c'} \tag{1}$$

Where, E_c is the modulus of elasticity (psi); and
f_c' is the 28-day compressive strength (psi).

Target Segment Element (TARGE170)

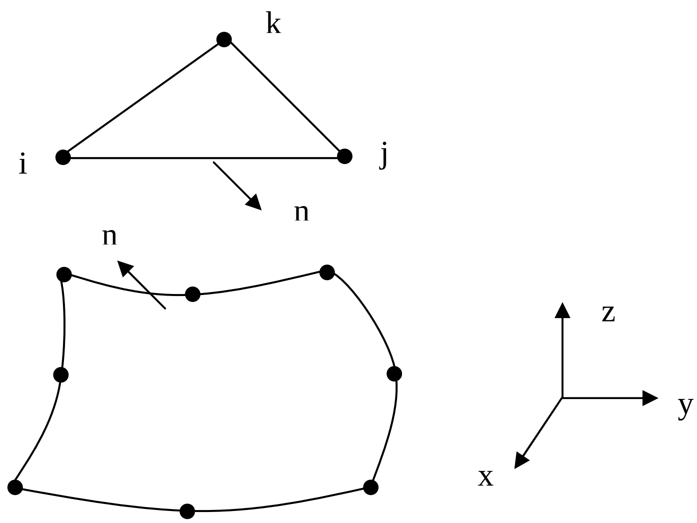

Surface-to-Surface Contact Element (CONTA174)

Figure 4. Geometry and Node Locations for CONTA174 Element

Modulus of elasticity of the concrete and BDB layers used in FE modeling varied from 25.4 to 32.1 GPa and 4.5 and 10.1 GPa, respectively. Literature shows that the modulus of elasticity of the lime-treated subgrade varies from 138 to 480 MPa (20,000 to 70,000 psi) (CDOT, 2003). For this study, subgrade modulus of elasticity was taken as 276 MPa (40,000 psi) for all models. Poisson's ratios for the concrete, BDB, and lime-treated subgrade layers were assumed to be 0.15, 0.15, and 0.20, respectively. The modulus of elasticity and the Poisson's ratio for the dowel bars were assumed as 200 GPa (29×10^6 psi) and 0.25, respectively. The typical values of 9×10^{-6} microstrains/°C (5×10^{-6} in/in/°F) and 12×10^{-6} microstrains/°C (6.5×10^{-6} in/in/°F) were used as the coefficients of thermal expansion for concrete and steel, respectively.

Mesh Building and Loading

Building an FE mesh is an important part of FE modeling. Finer meshes produce better results. However, several factors, such as, size and complexity of the geometry, use of contact elements, and product limitation of the ANSYS version used in this study, restricted the creation of a very fine mesh. Figure 5 shows the meshed geometry of a typical study section. In general, the mesh is coarse. However, because of discontinuities created by the joints in the slab, areas near the joints were refined to obtain better results. The total number of elements generated for each model was approximately 30,000.

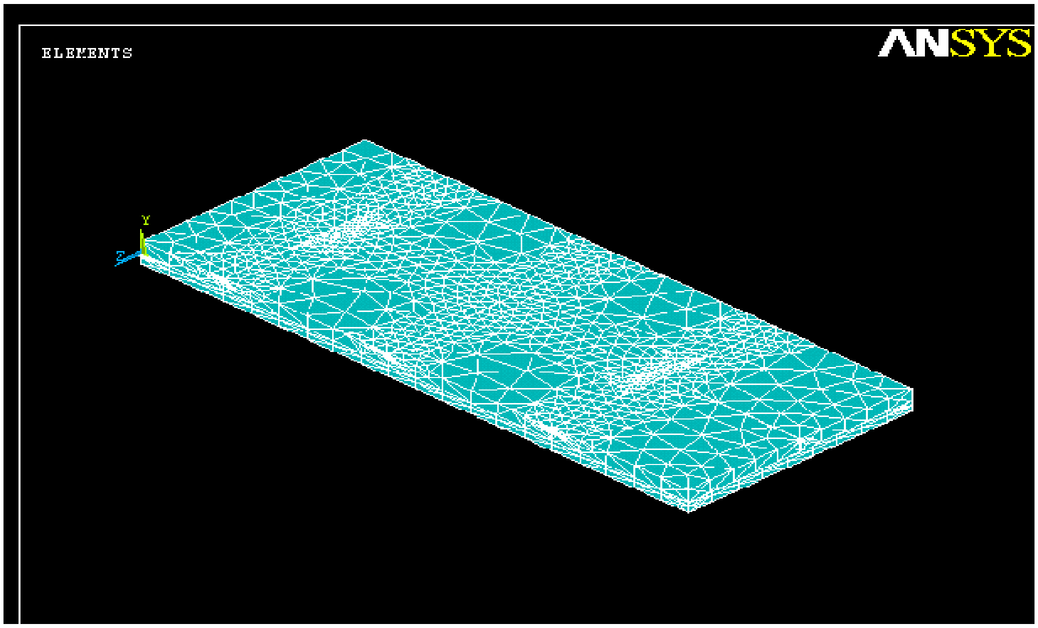

Figure 5. Mesh Geometry

In this study, temperature was used as the main load. Temperature data was applied at the top and bottom of the concrete slab with the assumption that the temperature distribution across the slab thickness is linear. The bottom of the subgrade layer was assumed to be fixed in all directions. The edges of the base and subgrade layers were fixed in the z-direction (direction of traffic). Pavement edge was allowed to move in all directions. Both translation and rotation of the dowel bar were restrained in all directions on one side of the joint.

FE Analysis Results

A positive and a negative temperature gradient simulating day and night time temperature differentials were applied to each modeled section. Table 2 shows the applied temperature differentials for the day and night times for all sections. As expected, pavement slabs curled downward and upward for the positive and negative temperature differentials, respectively. In this study, positive temperature differential refers to the daytime condition when temperature of the slab surface is higher than that of the bottom surface. The opposite is true for the negative temperature differential. Figures 6 and 7 show typical curled profiles of Section 6 for the positive and negative temperature differentials, respectively. These profiles were obtained in the longitudinal direction of the driving lane (direction of traffic) at a distance of 1 m (3 ft) from the outer edge of the driving lane (representing the right wheel path). Curling deflections in Figures 6 and 7 were obtained for temperature differentials of +5.6°C (+10°F) and –5.0°C (–9°F), respectively. Although the magnitudes of positive and negative temperature differentials are close, the magnitude of the maximum curling deflection varied. The maximum curling deflection for the positive temperature differential is slightly higher than that for the negative temperature differential. Similar observations were made in other simulation runs.

Table 2. Applied Pavement Temperatures Differentials

Section	Temperature Differential (^{0}C)	
	Daytime	Nighttime
1	13.9	-16.7
2	7.2	-6.7
3	19.4	-15
4	11.1	-5.5
5	12.2	-6.7
6	5.5	-5
7	8.3	-8.3
8	3.9	-2.8
9	16.1	-10.6
10	8.3	-4.4
11	15.0	9.5
12	6.7	3.9

Table 3 tabulates the maximum downward and upward curling deflection values for all test sections. Positive deflection value represents the maximum downward curling deflection and vice versa. Maximum downward curling deflection values for Sections 3 and 9 are higher compared to other sections. Temperature differential values applied on these sections were much higher compared to other sections. Slab thickness of these sections is also lower than other sections. On the other hand, for upward curling, maximum curling deflection values were obtained for Section 1 that has the highest slab thickness. Curling profiles of the right and left wheel paths were not exactly the same. However, the difference is not significant.

Because of the continuity of the concrete pavement in the longitudinal direction, the deflection profile for all slabs should be the same provided all

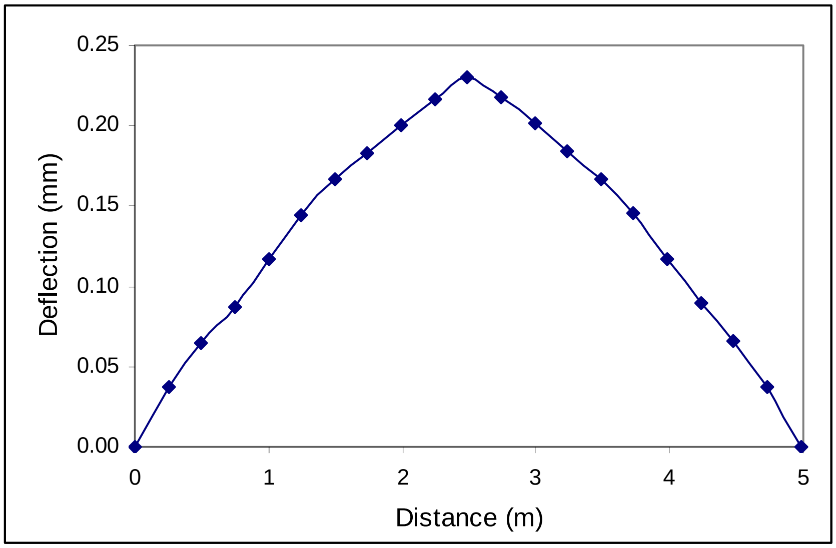

Figure 6 Curled Profile of Section 6 for Positive Temperature Differential

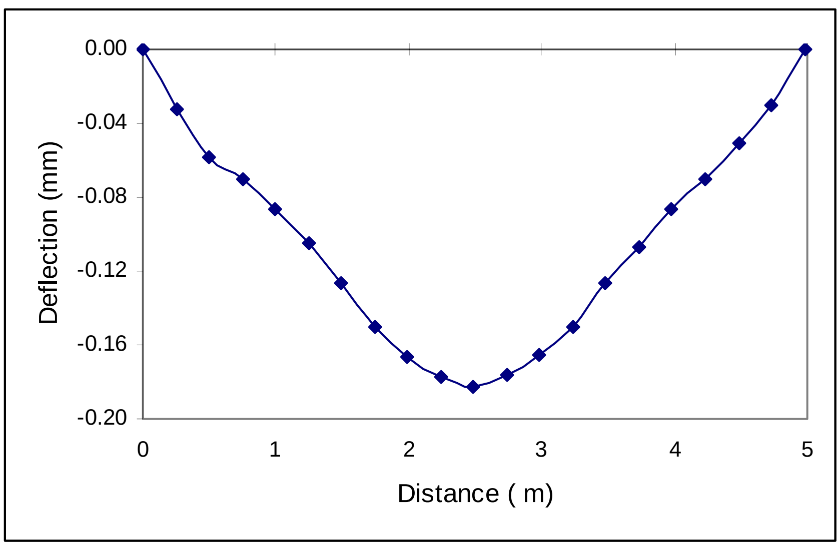

Figure 7 Curled Profile of Section 6 for Negative Temperature Differential

material properties, dimensions, and applied temperature loading of these slabs are the same. Based on this assumption, profile of each model resulting from the applied temperature differential was generated for 10 continuous slabs. Figure 8 shows a continuous profile for Section 6 resulting from a positive temperature differential. Roughness values, in terms of International Roughness Index (IRI), were calculated from all profiles resulting from curling. IRI is the most widely used parameter to

Table 3. Maximum Curling Deflections Obtained by FE Simulation

Test Section	Maximum Downward Curling Deflection (mm)		Maximum Upward Curling Deflection (mm)	
	Left Wheel Path	Right Wheel Path	Left Wheel Path	Right Wheel Path
1	0.312	0.312	-0.383	-0.387
2	0.241	0.241	-0.158	-0.158
3	0.426	0.426	-0.307	-0.310
4	0.303	0.305	-0.216	-0.218
5	0.376	0.378	-0.242	-0.244
6	0.230	0.230	-0.183	-0.185
7	0.291	0.295	-0.215	-0.215
8	0.221	0.222	-0.137	-0.137
9	0.407	0.409	-0.273	-0.275
10	0.305	0.307	-0.193	-0.194
11	0.404	0.408	-0.261	-0.256
12	0.278	0.278	-0.140	-0.140

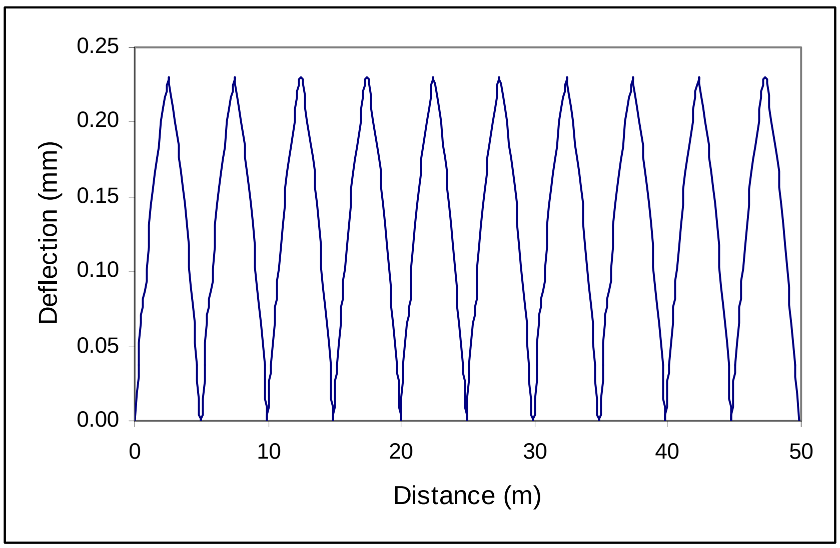

Figure 8. Deflection Profile for 10 Continuous Slabs

represent road roughness. The IRI has a unit of slope i.e. m/km or in/mi. IRI values were calculated using RoadRuf software developed by the University of Michigan Transportation Research Institute. RoadRuf uses profile of a given length of pavement section to calculate the IRI values. Table 4 tabulates the IRI values for the curled profiles of different sections. The IRI values are very consistent with the maximum deflections presented in Table 3. Like the maximum curling deflection values, differences in the IRI values for the left and right wheel paths for a given simulation model is negligible.

Table 4. IRI Values (m/km) Resulting from Curled Profiles

Section	Downward Curling		Upward Curling	
	Left Wheel Path	Right Wheel Path	Left Wheel Path	Right Wheel Path
1	0.122	0.124	0.145	0.147
2	0.094	0.095	0.058	0.059
3	0.157	0.166	0.100	0.101
4	0.118	0.118	0.083	0.084
5	0.133	0.137	0.094	0.096
6	0.088	0.093	0.070	0.072
7	0.115	0.117	0.079	0.079
8	0.084	0.086	0.051	0.051
9	0.154	0.157	0.102	0.105
10	0.119	0.121	0.072	0.074
11	0.154	0.160	0.098	0.100
12	0.108	0.109	0.053	0.053

Statistical Analysis

Regression analysis was preformed to find the relationship between curling and various factors that were used as variables in the models. Separate regression models were developed for the maximum curling deflection and the IRI values obtained from the curled profiles of the simulated pavement sections. The analysis was performed using SAS software (SAS, 1999).

Curling Deflection Model

The response variable for this model is the maximum curling deflection (in mils) that occurs at the middle of the wheel paths of the slab. Predictor variables used for this model development are: slab thickness, 28-day compressive strength of the concrete slab, 28-day compressive strength of the BDB layer, and temperature differential between the pavement top and bottom surfaces. Based on the scatter plots of the response variables against the predictor variables, it was decided that multiple linear regression would be appropriate to describe the relationship between the response and predictor variables. The correlations (or multicollinearity) among the predictor variables were evaluated by the scatter plots of these variables and by the variance inflation factor (VIF) values. No correlation was found among the predictor variables. As mentioned earlier, depending upon the temperature gradient, pavement slabs curl upward or downward. Since both types of curling were simulated, first it was checked to see whether separate models were needed to represent each type of curling or a single model can represent both. To check this, a full model was run using results obtained for both upward and downward curling. Type of curling was used as a categorical variable. Then full model was compared against the models developed for different levels of categorical variables to find whether a single model could be used for all categorical variables. Statistical analysis results showed that separate models were needed for the downward and upward curling. Thus separate models were developed for downward and upward curling .

The model for downward curling is shown in Equation 2:

$$DCDef = 11.38112 - 0.23978H - 0.000635 f_c^{/} + 0.00379 BDBf_c^{/} + 0.31892 \Delta TPOS$$

with SSE = 9.01; RMSE = 1.135; R^2 = 0.898; adjusted R^2 = 0.839. (2)

where, DCDef is the downward curling deflection (mils);

H is the slab thickness (inch);

$f_c^{/}$ is the 28-day compressive strength of concrete (psi);

$BDBf_c^{/}$ is the 28-day compressive strength of BDB (psi); and

$\Delta TPOS$ is the absolute temperature differential between the pavement top and bottom when the pavement top is warmer than the bottom (^{0}F).

The equation reveals that with an increase in temperature differential and 28-day compressive strength of the BDB layer, maximum downward deflection value increases. However, maximum downward curling deflection decreases with an increase in slab thickness and 28-day compressive strength of the concrete slab.

Equation 3 presents the model for upward curling that happens when temperature at the top of the concrete slab is lower than that for the bottom:

$$UCDef = 8.07247 - 0.1307H - 0.000789 f_c^{/} + 0.00555 BDBf_c^{/} + 0.33382 \Delta TNEG$$

with SSE=14.56; RMSE = 1.457; R^2 =0.818; adjusted R^2 = 0.714. (3)

where, UCDef is the upward curling deflection (mils); and

$\Delta TNEG$ is the absolute temperature differential between the pavement top and bottom when the top is cooler than the bottom (^{0}F).

The equation indicates that for a given section, upward curling will reach a maximum value when the negative temperature differential is maximum, which usually happens sometime in the morning.

IRI Model

For this model, the response variable is the International Roughness Index (IRI) (in in/mi) computed from the curled profile of the pavement slabs. Predictor variables used are the same as those used in the curling deflection model. The value of IRI is always positive, although the elevation points of the profiles can be positive or negative depending upon the time of the day. Like the curling deflection model, it was first checked whether the IRI obtained from both upward and downward curled profiles can be described with a single model or separate models are needed. Analysis by SAS revealed that separate models were needed for the IRI values computed from the upward and downward curled profiles. Equation 4 shows the model developed for the IRI values calculated from the profiles generated due to downward curling:

$$IRIDC = 7.8485 - 0.21048H - 0.000266 f_c^/ + 0.00088 BDBf_c^/ + 0.1802\Delta TPOS$$

with SSE = 2.784; RMSE = 0.631; R^2 = 0.907; adjusted R^2 = 0.853. (4)

where, IRIDC is the IRI values calculated from the profiles of concrete slab due to downward curling (in/mi).

Equation 4 presents the model obtained for the IRI values corresponding to the profiles when the pavements experienced negative temperature differential:

$$IRIUC = 4.5568 - 0.10156H - 0.000355 f_c^/ + 0.00322 BDBf_c^/ + 0.20622\Delta TNEG$$

with SSE = 5.45; RMSE = 0.882; R^2 =0.827; adjusted R^2 = 0.728. (5)

where, IRIUC is the IRI value resulting from the profiles of the concrete slab due to upward curling (in/mi).

These models are very similar to those obtained for curling deflection. Only the coefficients of the parameter estimates are different. For this parameter, with an increase in temperature differential and 28-day compressive strength of the BDB layer, IRI due to maximum downward or upward curling would increase. However, IRI due to maximum downward or upward curling would decrease with an increase in slab thickness and 28-day compressive strength of the concrete slab.

The IRI scale is linearly correlated with the roughness or profile elevations points that cause roughness. If all elevations of a measured profile increase, then the IRI value would increase proportionately. The curled profiles of different sections obtained from the FE simulations are similar in shape but different in magnitude. Profiles with higher elevation values will result in higher IRI and vice versa.

Conclusions

Three-dimensional Finite Element (FE) simulation results of curling of Portland Cement Concrete Pavements (PCCP) have been presented in this paper. The simulation was done with commercially available FE software, ANSYS. Based on the study, the following conclusions can be drawn:

- Curling deflections and the IRI values resulting from curled profiles are affected by the concrete slab thickness, 28-day compressive strength of concrete, 28-day compressive strength of the BDB layer, and the temperature differential between the pavement top and bottom.
- Higher temperature differential increases both upward and downward curling as well as IRI values resulting from the profiles of the curled slabs. The magnitude of curling deflection resulting from a particular positive

temperature differential is slightly higher than that resulting from a negative temperature differential with the same magnitude.

- Material properties that influence curling include 28-day compressive strength of the concrete and BDB layers. Higher concrete slab compressive strength tends to decrease both upward and downward curling. However, the relationship between the BDB compressive strength and curling is opposite, i.e., curling will increase with an increase in BDB compressive strength.
- Lower curling and IRI values were observed for slabs with higher thickness.

Acknowledgement

The authors wish to thank Dr. Xiao Xin, Dr. Stefan Romanoschi, and Dr. Jeff Pontius of Kansas State University for their help during various stages of this study. Mr. Bryce Barkus and Mr. Aneel Gogula, formerly with Kansas State University, helped during temperature data collection. Their cooperation in this study is hereby acknowledged.

References

American Concrete Institute (ACI) (1986). *Building Code Requirements for Reinforced Concrete*, ACI Committee 318 Report, ACI 318-83, Farmington Hills, Michigan.

ANSYS (2003). *Structural Analysis Guide*, ANSYS, Inc., Pennsylvania.

Byrum, C. R (2000). "Analysis of LTPP JCP Slab Curvature Using High Speed Profiles." *Transportation Research Record No. 1730*, Transportation Research Board, National Research Council, Washington D.C., 1-9.

Channnakeshava, C., Barzegar, F., and Voyiadjis, G. Z. (1993). "Nonlinear FE Analysis of Concrete Pavements with Doweled Joints.", *Journal of Transportation Engineering*, ASCE, Vol. 119, No. 5, September/October, 763-781.

Chatti, K., Lysmer, J., and Monismith, C. L. (1994). "Dynamic Finite-Element Analysis of Jointed Concrete Pavement." T*ransportation Research Record 1449*, Transportation Research Board, National Research council, Washington, D.C., 79-90.

Chou, Y. T. (1981). *Structural Analysis Computer Programs for Rigid Multicomponent Pavement Structures With Discontinuities: WESLIQID and WESLAYER*, Technical Report GL 81-6. U.S. Army Engineer Waterways Experiment Station, Vicksburg, Mississippi.

Colorado Department of Transportation (CDOT). *Colorado DOT Pavement Design Manual*, <http://www.codot.org> (Sept, 2003).

Davis, W. G., Turkiyyah, G. M., and Mahoney, J. P. (1998). "EverFE: Rigid Pavement Three-Dimensional Finite Element Analysis Tool." *Transportation Research Record 1629*, Transportation Research Board, National Research Council, Washington, D.C., 41-49.

Huang, Y. H. (1993). *Pavement Analysis and Design*, Prentice Hall, Inc., New Jersey.

Kuo, C. M. (1994). *Three-Dimensional Finite Element Analysis of Concrete Pavement*, Ph.D. Dissertation, University of Illinois, Urbana-Champaign, Illinois.

Parcells, Jr., W.H., and Hossain, M. (1994). "Kansas Experience with Smoothness Specifications for Concrete Pavements." *Transportation Research Record 1435*, Transportation Research Board, National Research Council, Washington, D.C., 115-123.

SAS (1999). *Statistical Analysis System*, The SAS Institute, Carey, North Carolina.

Saxena, S. K., and Dounias, G. T. (1986). "Mechanical and Environmental Stresses in Continuously Reinforced Concrete Pavements.", T*ransportation Research Record 1099*, Transportation Research Board, National Research Council, Washington, D.C., 12-21.

Tabatabaie, A. M., and Barrenberg, E. J. (1978). "Finite Element Analysis of Jointed or Cracked Concrete Pavements." T*ransportation Research Record 671*, Transportation Research Board, National Research Council, Washington, D.C., 11-17.

Tang, T., Zollinger, D. G., and Senadheera, S. (1993). "Analysis of Concave Curling in Concrete Slabs." *Journal of Transportation Engineering*, ASCE, Vol. 119, No. 4, Jul/Aug, 618-632.

Tayabji, S. D., and Colley, B. E. (1986). *Analysis of Jointed Concrete Pavements*, Technical Report FHWA-RD-86-041, Federal Highway Administration, U.S. Department of Transportation.

Uddin, W., Hackett, R. M., Joseph, A., Pan, Z., and Crawley, A. B. (1995). "Three-Dimensional Finite-Element Analysis of Jointed Concrete Pavement with Discontinuities." *Transportation Research Record 1482*, Transportation Research Board, National Research Council, Washington, D.C., 26-32.

Vepa, T. S., and George, K. P. (1997). "Deflection Response Models for Cracked Rigid Pavements." *Journal of Transportation Engineering*, ASCE, Vol. 123, No. 5, September/October, 377-384.

Yu, H. T., Smith, K. D., Darter, M. I., Jiang, J., and Khazanovich, L. (1998). *Performance of Concrete Pavements, Volume III: Improving Concrete Pavement Performance*, Report FHWA-RD-95-111, Federal Highway Administration, U.S. Department of Transportation.